Received February 2, 2020, accepted February 11, 2020, date of publication February 13, 2020, date of current version February 24, 2020.

*Digital Object Identifier 10.1109/ACCESS.2020.2973858*

# Design and Development of a Rayleigh Oscillator-Based Reference Angle Generator for Motion Control of Smart Prosthetic Knees

**LEI XU [1,3] AND QIANG FU [2,3]**

[1]Mechatronics Laboratory, Department of Automation, Shanxi University, Taiyuan 030006, China
[2]Department of Robot Engineering, Chongqing University of Arts and Sciences, Chongqing 402160, China
[3]Department of Optoelectronic Engineering, Chongqing University, Chongqing 400044, China

Corresponding author: Qiang Fu (qfu@cqwu.edu.cn)

**ABSTRACT** In order to synchronize the motions of the above-knee amputee's limbs and smart prosthetic knee in practical applications, the principle of a Rayleigh oscillator-based reference angle generator (RORAG) for the motion control of smart prosthetic knees is proposed. The central pattern generator (CPG) model of the lower limb in this paper uses a pair of phase-coupling Rayleigh oscillators to imitate the human's lower limb's biological CPG, where the used Rayleigh oscillators are improved to exactly represent the motion characteristics of the lower limb. A frequency control method for the CPG model is proposed to synchronize the thigh reference angle, which is generated by the lower limb's CPG model, with the swing angle of the above-knee amputee's residual thigh. The RORAG model is developed by using the real-time simulation system. An experimental system is developed to verify the performance of the RORAG model in two terms of the curve shape and motion synchronization. Further, in order to estimate the application value of the proposed RORAG model in two terms of the real-time and accuracy, a bio-guided motion platform system is developed and fabricated. On this motion platform system, the RORAG model is used to control a prosthetic knee prototype. The experimental results show that the developed RORAG model can imitate the subject's knee joint's swing angle accurately in real time. Therefore, the proposed RORAG is effective in practical applications.

**INDEX TERMS** Motion characteristics, reference angle generator, prosthetic knees, Rayleigh oscillator.

## I. INTRODUCTION

Synchronization with the amputee is a key fact to a smart prosthetic knee, because it determines the coordination of the prosthesis with the amputee. Therefore, the synchronized motion controlling of the smart prosthetic knee has been a popular research field since the last decades [1]–[4]. Compared with the finite state machine controlling methods [5], trajectory tracking control methods are widely applied on the lower limb prosthesis because of their synchronism with the amputee' motion [6]–[12]. In this case, the reference angle is an important factor to determining the motion performance of the smart prosthetic knee. Over the past few decades, some researchers have used the trajectory tracking control to control the smart prosthetic knee. For example, Wang *et al.* [6] and Akdogan *et al.* [7] proposed the computed torque and PD control for the smart prosthetic knee. Popovic and Kalanovic [8] applied Lyapunov direct method to the trajectory tracking control for the smart prosthetic knee. On this base, he proposed the optimal control further [9]. Kalanovic *et al.* [10] proposed the neural network and PD control method. Kim and Oh [11] proposed a combination control method by combining the iterative learning method with the computed torque and PD control method. As well, Scandaroli *et al.* [12] proposed the model reference adaptive control. The above mentioned control methods need the reference angle, which are currently obtained by fitting the pre-collecting data sets of the human's lower limb's swing angles, as the control target when controlling the smart prosthetic knee. Although the fitted reference angle can well imitate

The associate editor coordinating the review of this manuscript and approving it for publication was Zheng Chen.

the swing of the lower limb, they can only generate some limited reference angles, which makes it difficult to adjust the amplitude and frequency of the smart prosthetic knee's swing angle in real time in the walking process. Therefore, it can be imagined that the realization of a reference angle generator that reflects the motion characteristics of the human body's lower limb in the form of the control parameters, such as the amplitude, phase difference and frequency, will have important significance for the efficient control of the prosthetic knees.

Biological studies indicate that the amplitudes and frequencies of the rhythmic motions of organisms are adjusted by the central pattern generator (CPG), which is a kind of neural network distributed throughout the lower thoracic and lumbar regions of the spinal cord [13]–[15]. On these bases, to generate the adjustable reference angles for walking control, CPGs were introduced into the walking robot control strategies by some researchers. It is found that CPG has significant advantages such as self-excitation, phase interlock, and dynamic regulation parameters [14], [15]. For example, Conradt [16] designed a CPG model of the serpentine robot based on Kuramoto oscillator, which realized the crawling control in different environments. Morimoto *et al.* [17] designed a CPG model of the bipedal robot based on Hopf oscillator. Zielinska [18] designed a CPG model of the two-legged walking machine based on VDP oscillator. Torrealba *et al.* [19] used sines and cosines as the prosthesis' CPG model. We [20] also proposed a cardioid oscillator to model rhythmic motions with asymmetric time ratios in the CPG model. As a classic oscillator, Rayleigh oscillator is also used as CPG model. De Pina *et al.* [21] designed a CPG model of the bipedal robot based on Rayleigh oscillator. On this basis, Nandi *et al.* [22] established the mutual coupled CPG model to imitate the motions of the lower limb. Mondal *et al.* [23] optimized the parameters of the Rayleigh oscillator using Genetic algorithm to match an actual human locomotion captured by the intelligent gait oscillation detector biometric device. Kumar *et al.* [24] studied the phase difference between the oscillator entrained response and the external excitation in the case of a floor subjected to a harmonic lateral motion. Prakash *et al.* [25] proposed a hybrid Van der Pol–Duffing–Rayleigh oscillator to accurately represent the lateral force acting on a rigid floor due to human walking. And we [26] proposed a CPG-based coupling control method for synchronously controlling the two degrees of freedom robot based on the study for the Rayleigh oscillator's control parameters. These above mentioned CPG models, which are applied to the biped robots, imitate coordinated motion among the limb's joint via multiple Rayleigh oscillators. However, there are two problems when the CPG technology of the biped robot is applied to the human prosthesis. First, multiple control parameters of the Rayleigh oscillators have to be adjusted at the same time to change the curve shape of the reference angle of the biped robot. Due to the coupling relationship among the control parameters, both the amplitudes of the reference angles and the phase difference between the different reference angles are simultaneously affected by a single control parameter. Therefore, it is difficult to quickly obtain the curve shape of the reference angle to imitate the biological lower limb's motion characteristics through once adjustment for multiple control parameters of the Rayleigh oscillators. Second, unlike the biped robots, the above-knee amputee's remaining limbs are controlled by their own biological CPG, while not the established CPG model. Currently, the prosthetic knee's reference angle generated by the CPG model either does not take into account the synchronization with the limbs of the above-knee amputee, or uses the above-knee amputee's previous gait cycle time as its subsequent gait cycle time. But in the actual walking process, the current gait cycle time is not necessarily the same as the last gait cycle time, especially when the walking speed changes. Therefore, in the practical applications [27], [28], it is necessary not only to establish a CPG model that is easy to quickly adjust online, but also to consider the synchronization between the established CPG model and the above-knee amputee's biological limbs.

In order to solve the above problems, the principle of a Rayleigh oscillator-based reference angle generator (RORAG) for motion control of smart prosthetic knees is proposed. The specific contributions of this work are: (1) a reference angle generator, whose parameters are corresponding to the motion characteristics of the biological lower limb, is realized by improving a pair of phase-coupling Rayleigh oscillators. In the study, the values of the attenuation and coupling parameters ($\delta_1$, $c_1$, $\delta_2$, $c_2$) based on experimental experience, and the values of the amplitude control parameters ($q_1$, $q_2$) based on equation (6) are used to set the control parameters of the Rayleigh oscillators, so that the Rayleigh oscillators are controlled by only one frequency control parameter $\Omega_1$. Based on this empirical data set, the Rayleigh oscillators generate the stable curves. Then, based on the stable curves generated by the Rayleigh oscillators, the amplitude of the curve is adjusted according to equation (7). This method avoids multiple control parameters to be adjusted at the same time. Our proposed reference angle generator is stable and easy to implement, which is conducive for the practical applications; (2) the synchronization between the established CPG model and the above-knee amputee's limb's biological CPG is realized. A frequency control method for the lower limb's CPG model is proposed to match the frequency of the thigh reference angle generated by the CPG model with the swing frequency of the above-knee amputee's residual thigh; (3) the corresponding experimental system is specially developed and fabricated to verify the effectiveness of the proposed RORAG in practical applications. An experimental system is established to verify the RORAG model in two terms of the curve shape and motion synchronization. Further, a bio-guided motion platform system is developed and fabricated to verify the RORAG model in two terms of the real-time and accuracy.

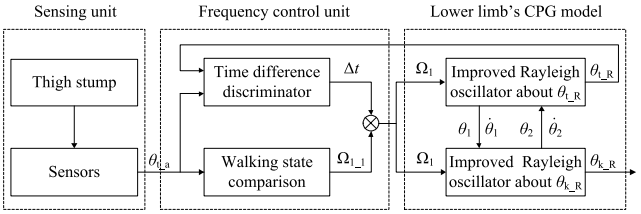


**FIGURE 1.** Block diagram of the RORAG.

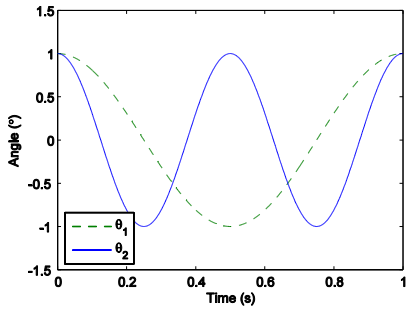


**FIGURE 2.** Time histories of the state variables $\theta_1$ and $\theta_2$.

## II. PRINCIPLE

The block diagram of the proposed RORAG is shown in Figure 1. According to Figure 1, the RORAG is composed of a lower limb's CPG model, a sensing unit, and a frequency control unit. The lower limb's CPG model is established by using a pair of phase-coupling Rayleigh oscillators, whose parameters can imitate the motion characteristics of the biological lower limb. The sensing unit is used to measure the thigh's swing angle. The frequency control unit controls the frequency control parameters of the CPG model to synchronize with the swing frequency of the above-knee amputee's residual thigh.

### A. LOWER LIMB'S CPG MODEL

In this study, the lower limb's CPG model uses a pair of phase-coupling Rayleigh oscillators [21], [22] to imitate the swing angles of the thigh and knee joint. The phase-coupling Rayleigh oscillators can be expressed as

$$\begin{cases} \ddot{\theta}_1 - \delta_1 \left(1 - q_1 \dot{\theta}_1^2\right) \dot{\theta}_1 + \Omega_1^2 \theta_1 - c_1 \dot{\theta}_2 \theta_2 = 0 \\ \ddot{\theta}_2 - \delta_2 \left(1 - q_2 \dot{\theta}_2^2\right) \dot{\theta}_2 + \Omega_2^2 \theta_2 - c_2 \dot{\theta}_1 \theta_1 = 0 \end{cases} \tag{1}$$

where $\theta_i$ $(i = 1, 2)$ is the state variable generated by the $i$th $(i = 1, 2)$ Rayleigh oscillator; $\Omega_i$ $(i = 1, 2)$ is the frequency control parameter of the state variable $\theta_i$; $q_i$ $(i = 1, 2)$ is the amplitude control parameter of the state variable $\theta_i$; $\delta_i$ $(i = 1, 2)$ is the attenuation parameter of the state variable $\theta_i$; and $c_i$ $(i = 1, 2)$ is the coupling parameter between two Rayleigh oscillators.

When $\Omega_2 = 2\Omega_1 = 4\pi$, $q_1 = 4q_2 = 1/3\pi^2$, $\delta_1 = 0.1$, $c_1 = 0.0001$, $\delta_2 = 0.1$, $c_2 = 0.0001$, the time histories of the state variables $\theta_1$ and $\theta_2$ are shown in Figure 2. In Figure 2, the curve shape of the two state variables are approximately cosine waves with a frequency ratio of about 1:2. Therefore,

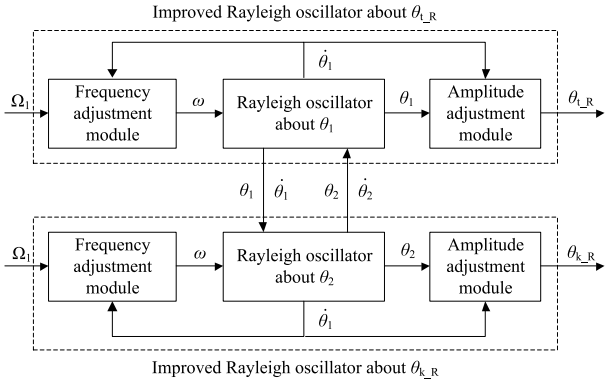


**FIGURE 3.** Block diagram of the improved Rayleigh oscillators.

it is assumed that the mathematical expressions of the desired state variables $\theta_1$ and $\theta_2$ are

$$\begin{cases} \theta_1 = A_1 \cos(\omega t) \\ \theta_2 = A_2 \cos(2\omega t) \end{cases} \tag{2}$$

where $A_1$ and $A_2$ are respectively the amplitude of the state variables $\theta_1$ and $\theta_2$; and $\omega$ is the gait frequency.

Substituting equation (2) into equation (1), we can get

$$\begin{cases} \Omega_1^2 A_1 \cos(\omega t) + \delta_1 \omega A_1 \sin(\omega t) \\ + c_1 \omega A_2^2 \sin(4\omega t) + \delta_1 q_1 \omega^3 A_1^3 \sin(3\omega t)/4 \\ = \omega^2 A_1 \cos(\omega t) + 3\delta_1 q_1 \omega^3 A_1^3 \sin(\omega t)/4 \\ \Omega_2^2 A_2 \cos(2\omega t) + \left(2\delta_2 \omega A_2 + c_2 \omega A_1^2/2\right) \sin(2\omega t) \\ + 2\delta_2 q_2 \omega^3 A_2^3 \sin(6\omega t) \\ = 4\omega^2 A_2 \cos(2\omega t) + 6\delta_2 q_2 \omega^3 A_2^3 \sin(2\omega t) \end{cases} \tag{3}$$

According to the harmonic balance method [29], the higher harmonics generated during the oscillation process are suppressed by the low-pass linear term in the oscillator. So the parameters $(q_i, \Omega_i)$ can be expressed as

$$\begin{cases} \Omega_1 = \omega \\ q_1 = 4/\left(3\omega^2 A_1^2\right) \\ \Omega_2 = 2\omega \\ q_2 = \left(4\delta_2 A_2 + c_2 A_1^2\right)/\left(12\delta_2 \omega^2 A_2^3\right) \end{cases} \tag{4}$$

According to equation (4), the frequency control parameters $\Omega_i$ can be determined by the gait frequency $\omega$, and the amplitude control parameters qi can be determined by the attenuation parameter $\delta_2$ and the coupling parameter $c_2$.

Figure 3 shows the block diagram of the improved Rayleigh oscillators based on the motion characteristics of the lower limb. In Figure 3, the Rayleigh oscillators are improved through the frequency adjustment module and the amplitude adjustment module. Through the frequency control parameter $\Omega_i$, the frequency adjustment module adjusts the corresponding gait frequency $\omega$, thereby the frequencies of the state variables $\theta_1$ and $\theta_2$ are adjusted in real time. Then, through the amplitude control parameter qi, the amplitude

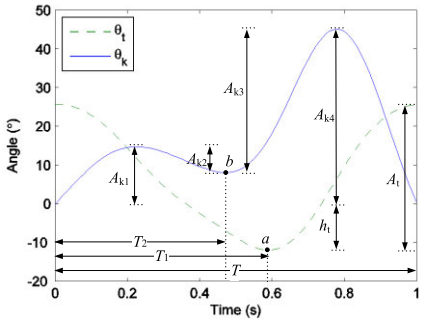


**FIGURE 4.** Time histories of the human's thigh's swing angle ($\theta_t$) and the knee joint's swing angle ($\theta_k$). (Point a, which is the pole of the thigh's angle, is considered as the cut-off point between the stance phase and the swing phase. Point b is the pole of the knee joint's angle. $A_t$ is the amplitude of the thigh's angle. $A_{k1}$ is the amplitude of the knee joint's angle when the knee joint is bent during the stance phase. $A_{k2}$ is the amplitude of the knee joint's angle when the knee joint is stretched during the stance phase. $A_{k3}$ is the amplitude of the knee joint's angle when the knee joint is bent during the swing phase, $A_{k4}$ is the amplitude of the knee joint's angle when the knee joint is stretched during the swing phase, and $T$ is the gait cycle time.).

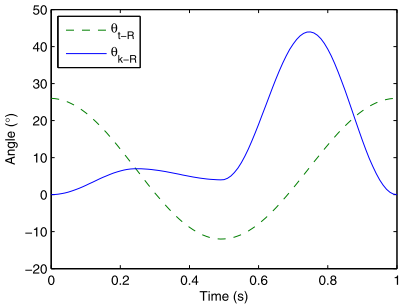


**FIGURE 5.** Time histories of the thigh reference angle ($\theta_{t\_R}$) and knee joint reference angle ($\theta_{k\_R}$) generated by the improved Rayleigh oscillators.

adjustment module adjusts the amplitudes of the state variables $\theta_1$ and $\theta_2$, and finally generates the thigh reference angle ($\theta_{t\_R}$) and the knee joint reference angle ($\theta_{k\_R}$).

In order to generate the reference angle that imitates the motion characteristics of the thigh and knee joint, the relevant control parameters of the Rayleigh oscillators need to be set according to the motion characteristics of the lower limbs. The time histories of the human's thigh's swing angle ($\theta_t$) and the knee joint's swing angle ($\theta_k$) are shown as Figure 4. As shown in Figure 4, the motion characteristics of the subject's lower limb can be reflected in the form of the parameters. Therefore, for different objects or different walking modes, the motion characteristics of the lower limbs can be extracted in the form of parameters ($A_t, A_{k1}, A_{k2}, A_{k3}, A_{k4}, T$) according to Figure 4. According to the value of the extracted lower limb's motion characteristic parameters, the control parameters of the Rayleigh oscillator can be set as follows.

According to the human knee joint's motion characteristics $T$ and $T_2$ in Figure 4, the frequency control parameters of the Rayleigh oscillator can be set to

$$\begin{cases} \Omega_2 = 2\Omega_1 = 2\omega = 2\pi/T_2, & \dot{\theta}_1 \le 0 \\ \Omega_2 = 2\Omega_1 = 2\omega = 2\pi/(T - T_2), & \dot{\theta}_1 > 0 \end{cases} \tag{5}$$

When $A_1 = 1, A_2 = 1, \delta_1 = \delta_2 = 0.1, c_1 = c_2 = 0.0001$, the amplitude control parameters of Rayleigh oscillator can be set to

$$\begin{cases} q_1 = (4T_2^2)/(3\pi^2), & \dot{\theta}_1 \le 0 \\ q_1 = (4(T - T_2)^2)/(3\pi^2), & \dot{\theta}_1 > 0 \\ q_2 = (4001T_2^2)/(12000\pi^2), & \dot{\theta}_1 \le 0 \\ q_2 = (4001(T - T_2)^2)/(12000\pi^2), & \dot{\theta}_1 > 0 \end{cases} \tag{6}$$

Based on the motion characteristics of the lower limb, the amplitudes of the state variables $\theta_1$ and $\theta_2$ are adjusted by the amplitude adjustment module, so we can get

$$\begin{cases} \theta_{t\_R} = A_t\theta_1 + \dfrac{A_t}{2} - h_t \\ \theta_{k\_R} = -A_{k1}\theta_1 + \dfrac{A_{k1}}{2}, & \dot{\theta}_1 \le 0\ \dot{\theta}_2 \le 0 \\ \theta_{k\_R} = -A_{k2}\theta_1 + A_{k1} - \dfrac{A_{k2}}{2}, & \dot{\theta}_1 \le 0\ \dot{\theta}_2 > 0 \\ \theta_{k\_R} = -A_{k3}\theta_1 + A_{k4} - \dfrac{A_{k3}}{2}, & \dot{\theta}_1 > 0\ \dot{\theta}_2 \le 0 \\ \theta_{k\_R} = -A_{k4}\theta_1 + \dfrac{A_{k4}}{2}, & \dot{\theta}_1 > 0\ \dot{\theta}_2 > 0 \\ A_{k4} = A_{k3} + A_{k1} - A_{k2}, & \textit{Contraint} \end{cases} \tag{7}$$

where $\dot{\theta}_1$ is the derivative of the state variable $\theta_1$; $\theta_{t\_R}$ is the thigh reference angle; and $\theta_{k\_R}$ is the knee joint reference angle. Based on equations (5), (6), and (7), the time histories of the thigh reference angle ($\theta_{t\_R}$) and knee joint reference angle ($\theta_{k\_R}$) generated by the improved Rayleigh oscillator are shown in Figure 5. In order to verify the effectiveness of the improved Rayleigh oscillators in the term of the curve shape, the knee joint reference angle ($\theta_{k\_R}$) generated by the improved Rayleigh oscillator is compared with the actual subject's knee joint's swing angle ($\theta_{k\_a}$) in Figures 8 and 9 of Section III-B1. In addition, in Figures 15-20 of Section IV-B, the effectiveness of the reference angle generator model is further verified in the practical applications.

### B. FREQUENCY CONTROL UNIT

According to Figure 3, the Rayleigh oscillator needs to set the frequency control parameter $\Omega_i$ and the amplitude control parameter $q_i$. According to the biological studies [13]–[15], not only a human being's various limbs can coordinate their motions in a stable manner, but also the swing amplitude of the limbs is basically stable under the control of the biological CPG. Therefore, the amplitude control parameter qi can be measured according to the specific prosthetic wearer. When the empirical data are used to set the control parameters of the Rayleigh oscillators, the phase difference between the knee joint reference angle ($\theta_{k\_R}$) and the thigh reference angle ($\theta_{t\_R}$) is interlocked. Therefore, based on the phase-interlocking relationship of the lower limb's CPG model, the synchronization between the knee joint reference angle ($\theta_{k\_R}$) and the above-knee amputee's thigh stump's swing

angle ($\theta_{t\_a}$) can be converted to the synchronization between the thigh reference angle ($\theta_{t\_R}$) and the above-knee amputee's thigh stump's swing angle ($\theta_{t\_a}$). In order to solve the above mentioned problems, the frequency control method for the lower limb's CPG model is proposed. The frequency control method consists of two parts.

In the first part, the frequency control parameter $\Omega_i$ of the thigh reference angle ($\theta_{t\_R}$) in the current gait is adjusted in real time by comparing with the thigh stump's swing angle ($\theta_{t\_al}$) in the last gait. Based on the thigh stump's swing angle ($\theta_{t\_a}$) measured by the sensing unit, the change value ($\Delta\theta_{t\_a}$) of the swing angle within the sampling time can be obtained. Compared with the change value ($\Delta\theta_{t\_al}$) of the thigh stump's swing angle at the corresponding period of the last gait, the adjustment equation of the frequency control parameter $\Omega_{1-1}$ of the thigh reference angle ($\theta_{t\_R}$) can be obtained as

$$\Omega_{1\_1} = \begin{cases} \left(K_P\left(\Delta\theta_{t\_al} - \Delta\theta_{t\_a}\right) + K_D\left(\Delta\dot{\theta}_{t\_al} - \Delta\dot{\theta}_{t\_a}\right)\right)\Omega_{1\_al}, \\ \qquad \dot{\theta}_{t\_a} < 0 \\ \left(K_P\left(\Delta\theta_{t\_a} - \Delta\theta_{t\_al}\right) + K_D\left(\Delta\dot{\theta}_{t\_a} - \Delta\dot{\theta}_{t\_al}\right)\right)\Omega_{1\_al}, \\ \qquad \dot{\theta}_{t\_a} \geq 0 \end{cases} \tag{8}$$

where $\Omega_{1\_al}$ is the frequency control parameter in the last gait; $\Delta\dot{\theta}_{t\_a}$ is the angle velocity of the thigh stump within the sampling time of the current gait; $\Delta\dot{\theta}_{t\_al}$ is the angle velocity of the thigh stump at the corresponding period of the last gait; and $K_P$ and $K_D$ are proportionality coefficients. In the stance phase, $\Delta\theta_{t\_a}$ and $\Delta\theta_{t\_al}$ are both negative values. If $\Delta\theta_{t\_a}$ is smaller than $\Delta\theta_{t\_al}$, it means that the walking speed becomes faster. If $\Delta\theta_{t\_a}$ is larger than $\Delta\theta_{t\_al}$, it means that the walking speed becomes slower. In the swing phase, $\Delta\theta_{t\_a}$ and $\Delta\theta_{t\_al}$ are both positive values. If $\Delta\theta_{t\_a}$ is larger than $\Delta\theta_{t\_al}$, it means that the walking speed becomes faster. If $\Delta\theta_{t\_a}$ is smaller than $\Delta\theta_{t\_al}$, it means that the walking speed becomes slower.

In the second part, the end times of the thigh reference angle ($\theta_{t\_Rl}$) and thigh stump's swing angle ($\theta_{t\_al}$) in the last gait may be inconsistent, which will cause the start times of them in the subsequent gait are inconsistent, so the time difference ($\Delta t$) between them needs to be corrected. Considering that the curve shape of the thigh reference angle ($\theta_{t\_R}$) may be different from that of the thigh stump's swing angle ($\theta_{t\_a}$), the logical judgments of the start time and end time of the time difference ($\Delta t$) are shown in Figure 6.

As shown in Figure 6, 1 is used to indicate in the stance phase, and 0 is used to indicate in the swing phase. The judgment parameters ($A$ and $B$) are expressed as

$$\begin{cases} A = 1, & \dot{\theta}_{t\_a} \leq 0 \\ A = 0, & \dot{\theta}_{t\_a} > 0 \\ B = 1, & \dot{\theta}_{t\_R} \leq 0 \\ B = 0, & \dot{\theta}_{t\_R} > 0 \end{cases} \tag{9}$$

where $\dot{\theta}_{t\_a}$ is the derivative of the thigh stump's swing angle $\theta_{t\_a}$, which is used to distinguish the swing phase and stance phase of the thigh stump; and $\dot{\theta}_{t\_R}$ is the derivative of the thigh reference angle $\theta_{t\_R}$, which is used to distinguish the swing phase and stance phase of the thigh reference angle.

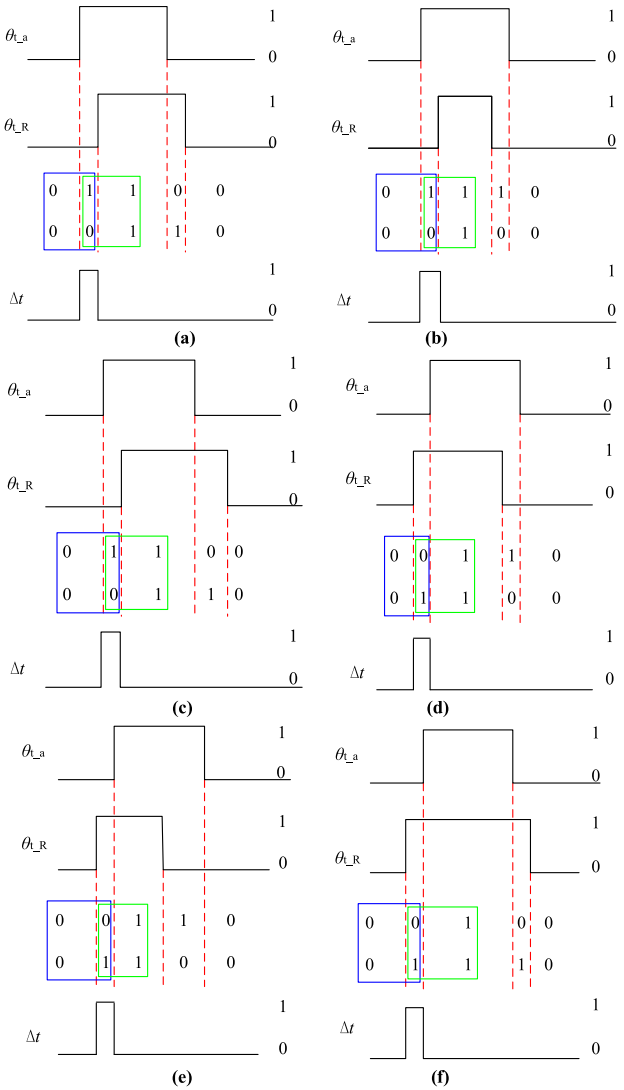


**FIGURE 6.** Logical judgments of the start time and end time of the time difference (Δt): (a) the time of the stance phase of the thigh reference angle ($\theta_{t\_R}$) is the same to that ($\theta_{t\_a}$) of the thigh stump in the acceleration state, (b) the time of the stance phase of the thigh reference angle ($\theta_{t\_R}$) is shorter than that ($\theta_{t\_a}$) of the thigh stump in the acceleration state, (c) the time of the stance phase of the thigh reference angle ($\theta_{t\_Rl}$) is longer than that ($\theta_{t\_a}$) of the thigh stump in the acceleration state, (d) the time of the stance phase of the thigh reference angle ($\theta_{t\_R}$) is the same to that ($\theta_{t\_a}$) of the thigh stump in the deceleration state, (e) the time of the stance phase of the thigh reference angle ($\theta_{t\_R}$) is shorter than that ($\theta_{t\_a}$) of the thigh stump in the deceleration state, and (f) the time of the stance phase of the thigh reference angle ($\theta_{t\_R}$) is longer than that ($\theta_{t\_a}$) of the thigh stump in the deceleration state.

The proposed logical judgments use a two-dimensional array $C = \{A, B\}$ for judging the start time and end time of the time difference ($\Delta t$). As shown in Figures 6(a), 6(b), and 6(c), the moment when $C$ changes from $\{0, 0\}$ to $\{1, 0\}$ is used as the start time of the time difference ($\Delta t$). The moment when $C$ changes from $\{1, 0\}$ to $\{1, 1\}$ is used as the end time of the

time difference ($\Delta t$). As shown in Figures 6(d), 6(e), and 6(f), the moment when $C$ changes from {0, 0} to {0, 1} is used as the start time of the time difference ($\Delta t$). The moment when $C$ changes {0, 1} to {1, 1} is used as the end time of the time difference ($\Delta t$).

According to the judged start time and end time, the value of the time difference ($\Delta t$) is calculated. As shown in Figures 6(a), 6(b), and 6(c), the thigh stump's swing angle ($\theta_{t\_a}$) is faster than the thigh reference angle ($\theta_{t\_R}$), thus the time difference ($\Delta t$) is a positive value. As shown in Figures 6(d), 6(e), and 6(f), the thigh stump's swing angle ($\theta_{t\_a}$) is slower than the thigh reference angle ($\theta_{t\_R}$), thus the time difference ($\Delta t$) is negative value. According to equations (8) and (9), the frequency control parameter $\Omega_1$ of the lower limb's CPG model is obtained as

$$\Omega_1 = \Omega_{1\_1} + K_t \Delta t \tag{10}$$

where $K_t$ is a proportionality coefficient. According to equation (10), the frequency control parameter $\Omega_1$ is adjusted in real time, so that the thigh reference angle ($\theta_{t\_R}$) is synchronized with the thigh stump's swing angle ($\theta_{t\_a}$).

## III. EXPERIMENTAL VERIFICATION

### A. EXPERIMENTAL SETUP

In order to experimentally verify the proposed RORAG in two terms of the curve shape and motion synchronization, the schematic diagram and the photograph of the experimental system are respectively shown in Figure 7(a) and 7(b) respectively. As shown in figure 7, an experimental setup is composed of a real-time simulation system, a subject, a sensing unit, a host computer and a motorized treadmill. The real-time simulation system (type: dSPACE DS1103 based on MATLAB/Simulink) is used to establish the RORAG model and acquire the signals through the 1st order Butterworth low-pass filter. The subject, who is a normal person, is used to provide the natural swing angles of the thigh and the knee joint. The sensing unit includes the angle sensor 1 and angle sensor 2. The angle sensor 1 (AS1, type: WDD35S2, linearity: 0.1%, Shanghai HuiRen Limited Company) is used to measure the angle of the subject's thigh. The angle sensor 2 (AS2, type: WDD35S2, linearity: 0.1%, Shanghai HuiRen Limited Company) is used to measure the angle of the subject's knee joint. The angle sensors (AS1 and AS2) are fixed to the subject by the hinge, whose first, second and third links are fixed to the subject's torso, thigh and shank, respectively. During assembly, the rotation centers of the angle sensors (AS1 and AS2) should be fixed coaxially to that of the subject's hip joint and knee joint, respectively. The motorized treadmill (type: KPT-460FA, China ShuHua Limited Company) is used to adjust the walking speed of the subject.

In experiments, the real-time simulation system accesses the signals measured by the angle sensors via its AD converter module. Then the measured signals are filtered by using 1st order Butterworth low-pass filter. According to the filtered signals of the subject's thigh and the established RORAG

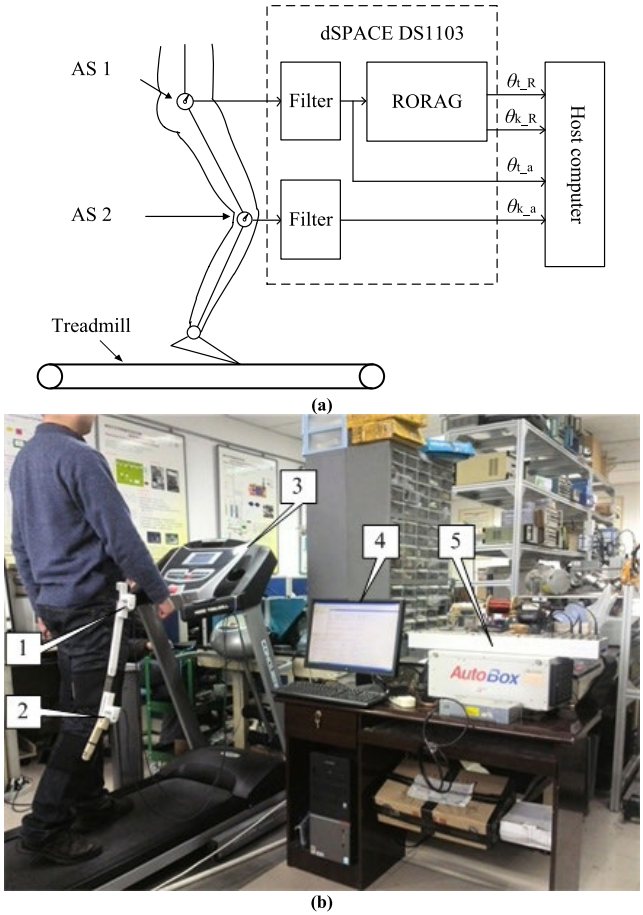


**FIGURE 7.** Experimental system: (a) the schematic diagram and (b) the photograph (1-angle sensor (AS1); 2-angle sensor (AS2); 3-motorized treadmill; 4-host computer; 5-dSPACE DS1103).

model, the thigh reference angle ($\theta_{t\_R}$) and knee joint reference angle ($\theta_{k\_R}$) is calculated, where a sampling frequency of 20 Hz is used to acquire the change value of the swing angle ($\Delta\theta_{t\_a}$) mentioned in Section II-B. Finally, the calculated thigh reference angle ($\theta_{t\_R}$) and knee joint reference angle ($\theta_{k\_R}$) by the RORAG model and the filtered swing angles ($\theta_{t\_a}$ and $\theta_{k\_a}$) of the subject's thigh and knee joint are collected by the real-time simulation system into the host computer for real-time display and record.

### B. EXPERIMENTAL RESULTS AND ANALYSIS

#### 1) CURVE SHAPE

The RORAG model is established by the real-time simulation system according to equations (5)-(7), and (10). When $A_{k1} = 10.5$, $A_{k2} = 2.5$, $A_{k3} = 36$, and $A_{k4} = 44$, the time histories of the knee joint reference angle ($\theta_{k\_R}$) generated by the RORAG model and the actual subject's knee joint's swing angle ($\theta_{k\_a}$) is shown in Figure 8, and the time history of the angle error between them is shown in Figure 9. In Figure 9, the maximum absolute angle error between the knee joint reference angle ($\theta_{k\_R}$) generated by the RORAG model and the actual subject's knee joint's swing angle ($\theta_{k\_a}$)

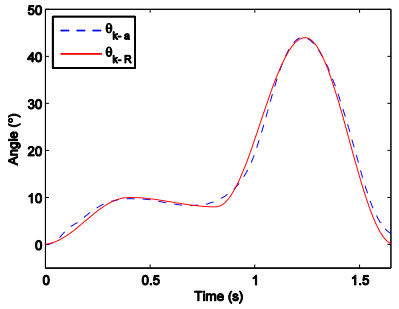


**FIGURE 8.** Time histories of the knee joint reference angle ($\theta_{k\_R}$) generated by the RORAG model and the actual subject's knee joint's swing angle ($\theta_{k\_a}$).

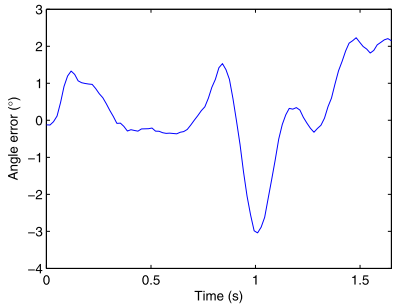


**FIGURE 9.** Time history of the angle error between the knee joint reference angle ($\theta_{k\_R}$) generated by the RORAG model and the actual subject's knee joint's swing angle ($\theta_{k\_a}$).

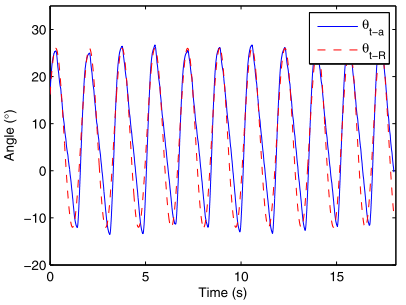


**FIGURE 10.** Time histories of the thigh reference angle ($\theta_{t\_R}$) generated by the RORAG model and the subject's thigh's swing angle ($\theta_{t\_a}$) in the first walking process.

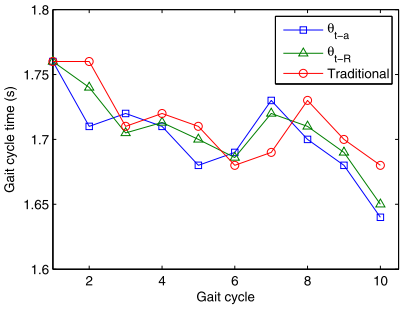


**FIGURE 11.** Gait cycle times of the thigh reference angle ($\theta_{t\_R}$) and the subject's thigh's swing angle ($\theta_{t\_a}$) in the first walking process.

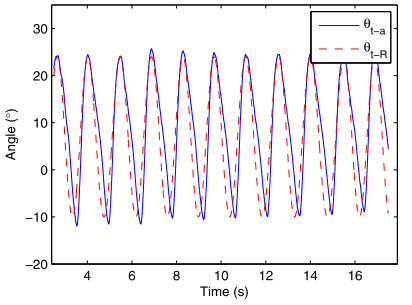


**FIGURE 12.** Time histories of the thigh reference angle ($\theta_{t\_R}$) generated by the RORAG model and the subject's thigh's swing angle ($\theta_{t\_a}$) in the second walking process.

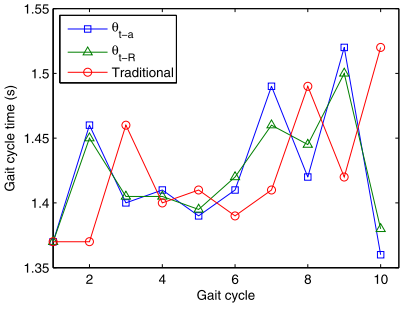


**FIGURE 13.** Gait cycle times of the thigh reference angle ($\theta_{t\_R}$) and the subject's thigh's swing angle ($\theta_{t\_a}$) in the second walking process.

is 3.04 °, the maximum relative angle error is 6.76 %, and the root mean square error (RMSE) is 1.21 °. The experimental result shows that the curve shape of the knee joint reference angle ($\theta_{k\_R}$) generated by the RORAG model can match with the motion characteristics of the actual subject's knee joint's swing angle ($\theta_{k\_a}$).

### 2) MOTION SYNCHRONIZATION

The subject performed two walking processes on the motorized treadmill, whose walking speeds are respectively from 0.85 m/s to 0.92 m/s and from 1.09 m/s to 0.98 m/s. In the first walking process, the time histories of the thigh reference angle ($\theta_{t\_R}$) generated by the RORAG model and the subject's thigh's swing angle ($\theta_{t\_a}$) are shown in Figure 10, and their gait cycle times are shown in Figure 11. In the second walking process, the time histories of the thigh reference angle ($\theta_{t\_R}$) generated by the RORAG model and the subject's thigh's swing angle ($\theta_{t\_a}$) are shown in Figure 12, and their gait cycle times are shown in Figure 13. The RMSEs, the maximum absolute errors, and the cumulative errors between the gait cycle time of the thigh reference angle ($\theta_{t\_R}$) and that of the subject's thigh's swing angle ($\theta_{t\_a}$) in two walking processes are shown in Table 1. In Figures 11, 13 and Table 1, the traditional method [20]–[23], [26] that uses the subject's previous gait cycle time as its subsequent gait cycle time is added for comparison. In Table 1, in the first walking process, the RMSE between the gait cycle time of the thigh reference angle ($\theta_{t\_R}$) and that of the subject's thigh's swing angle ($\theta_{t\_a}$) is 0.014 s, the maximum absolute error is 0.030 s,

**TABLE 1. RMSEs, max absolute errors, and accumulative errors between the gait cycle time of the thigh reference angle ($\theta_{t\_R}$) and that of the subject's thigh's swing angle ($\theta_{t\_a}$) in two walking processes.**

| | First walking process | | | Second walking process | | |
|---|---|---|---|---|---|---|
| | RMSE | Max absolute | Accumulative | RMSE | Max absolute | Accumulative |
| $\theta_{t\text{-}R}$ | 0.014s | 0.030s | 0.054s | 0.016s | 0.030s | 0.0035s |
| Traditional | 0.028s | 0.050s | 0.120s | 0.077s | 0.160s | 0.010s |

and the cumulative error is 0.054 s. The RMSE between the gait cycle time of the traditional method and that of the subject's thigh's swing angle ($\theta_{t\_a}$) is 0.028 s, the maximum absolute error is 0.050 s, and the cumulative error is 0.120 s. In the second walking process, the RMSE between the gait cycle time of the thigh reference angle ($\theta_{t\_R}$) and that of the subject's thigh's swing angle ($\theta_{t\_a}$) is 0.016 s, the maximum absolute error is 0.030 s, and the cumulative error is 0.0035 s. The RMSE between the gait cycle time of the traditional method and that of the subject's thigh's swing angle ($\theta_{t\_a}$) is 0.077 s, the maximum absolute error is 0.160 s, and the cumulative error is 0.010 s. The experimental results show that the proposed frequency control method is more effective than the traditional method. Using the proposed frequency control method, the curve shape of the knee joint reference angle ($\theta_{k\_R}$) can match with the motion characteristics of the subject's knee joint's swing angle ($\theta_{k\_a}$), and the thigh reference angle ($\theta_{t\_R}$) is synchronized with the subject's thigh's swing angle ($\theta_{t\_a}$).

## IV. APPLICATION VERIFICATION

### A. EXPERIMENTAL SETUP

In order to verify the effectiveness of the proposed RORAG in the application process, the schematic diagram and the photograph of the specially developed bio-guided motion platform system [30] are respectively shown in Figure 14(a) and 14(b). In Figure 14, the bio-guided motion platform system is composed of a real-time simulation system, a subject, a sensing unit, a host computer, a motorized treadmill, a motion platform, and a prosthetic knee prototype. The real-time simulation system, the subject, the sensing unit, the host computer, and the motorized treadmill are the same as described in Section III-A. The motion platform was developed and fabricated to imitate the swing of the subject's thigh. The main component of the motion platform is the thigh simulator, which is used to simulate the subject's thigh structure. The sensing unit is used to monitor the swing angles of the subject's thigh and knee joint in real time. In this experiment, a four-bar linkage prosthetic knee based on magnetorheological effect [31]–[33] developed in our laboratory is used as the prosthetic knee prototype. The developed prosthetic knee prototype [34] is mainly composed of the four-bar linkage and the integrated magnetorheological (MR) damper. The four-bar linkage is used to imitate the instantaneous center of the rotation of the subject's knee joint. The integrated MR damper, which is controlled by the controllable current driver (type:

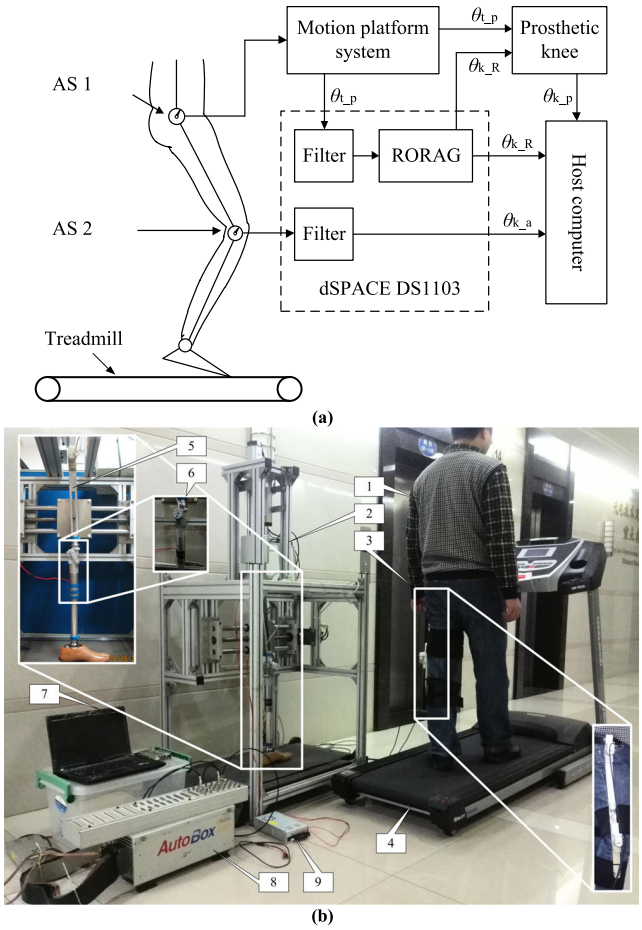


**FIGURE 14. Bio-guided motion platform system: (a) the schematic diagram and (b) photograph. (1-subject; 2-motion platform; 3-sensing unit; 4-motorized treadmill; 5-thigh simulator; 6-tested prosthetic knee prototype; 7-host computer; 8-dSPACE DS1103; and 9-controllable current driver).**

KH-10A, accuracy: 0.5 %, Wuhan ZHONGXING Company), is used to imitate the damping force of the subject's knee joint.

In experiments, on the one hand, according to the subject's thigh's swing angle ($\theta_{t\_a}$) monitored by the sensing unit, the thigh simulator's swing angle ($\theta_{t\_p}$) tracks the subject's thigh's swing angle ($\theta_{t\_a}$) in real time. According to the filtered thigh simulator's swing angle ($\theta_{t\_p}$) and the established RORAG model, the knee joint reference angle ($\theta_{k\_R}$) is calculated. On the other hand, the calculated knee joint reference angle ($\theta_{k\_R}$) is used as the reference angle of the prosthetic knee prototype. Driven by the thigh simulator, the prosthetic knee prototype's swing angle ($\theta_{k\_p}$) tracks the knee joint reference angle ($\theta_{k\_R}$) in real time. Finally, the knee joint reference angle ($\theta_{k\_R}$) generated by the RORAG model, the filtered subject's knee joint's swing angle ($\theta_{k\_a}$), and the prosthetic knee prototype's swing angle ($\theta_{k\_p}$) are all collected by the real-time simulation system into the host computer for real-time display and record.

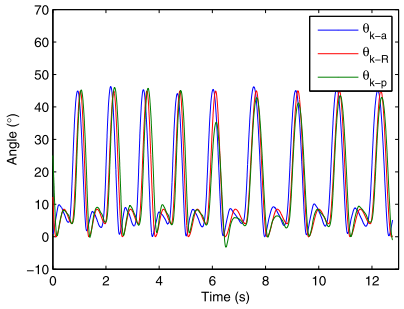


**FIGURE 15.** Time histories of the subject's knee joint's swing angle ($\theta_{k\_a}$), the knee joint reference angle ($\theta_{k\_R}$), and the prosthetic knee prototype's swing angle ($\theta_{k\_p}$) in the first walking process.

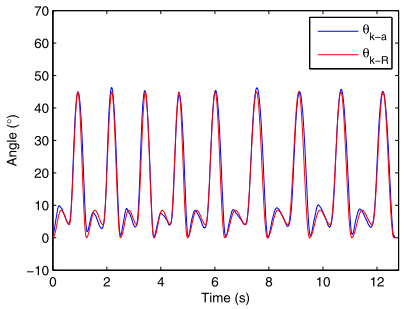


**FIGURE 16.** Time histories of the subject's knee joint's swing angle ($\theta_{k\_a}$) and the knee joint reference angle ($\theta_{k\_R}$) when ignoring the delay time in the first walking process.

### B. EXPERIMENTAL RESULTS AND ANALYSIS

The subject performed two walking processes on the motorized treadmill, whose walking speeds are respectively from 1.22 m/s to 0.95 m/s and from 0.78 m/s to 1.14 m/s. In the first walking process, the time histories of the subject's knee joint's swing angle ($\theta_{k\_a}$), the knee joint reference angle ($\theta_{k\_R}$) generated by the RORAG model, and the prosthetic knee prototype's swing angle ($\theta_{k\_p}$) are shown in Figure 15. The time histories of the subject's knee joint's swing angle ($\theta_{k\_a}$) and the knee joint reference angle ($\theta_{k\_R}$) when ignoring the delay time are shown in Figure 16, and the time history of the angle error between them is shown in Figure 17. In the second walking process, the time histories of the subject's knee joint's swing angle ($\theta_{k\_a}$), the knee joint reference angle ($\theta_{k\_R}$), and the prosthetic knee prototype's swing angle ($\theta_{k\_p}$) are shown in Figure 18. The time histories of the subject's knee joint's swing angle ($\theta_{k\_a}$) and the knee joint reference angle ($\theta_{k\_R}$) when ignoring the delay time are shown in Figure 19, and the time history of the angle error between them is shown in Figure 20.

According to Figures 15 and 18, the delay time between the subject's knee joint's swing angle ($\theta_{k\_a}$) and the knee joint reference angle ($\theta_{k\_R}$) is about 0.096 s. Consider the delay time (about 0.080 s) between the subject's thigh's swing angle ($\theta_{t\_a}$) and the thigh simulator's swing angle ($\theta_{t\_p}$) [30], the delay time between the thigh simulator's swing angle ($\theta_{t\_p}$) and the knee joint reference angle ($\theta_{k\_R}$) is about

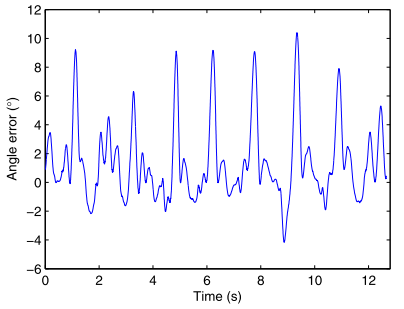


**FIGURE 17.** Time histories of the angle error between the subject's knee joint's swing angle ($\theta_{k\_a}$) and the knee joint reference angle ($\theta_{k\_R}$) in the first walking process.

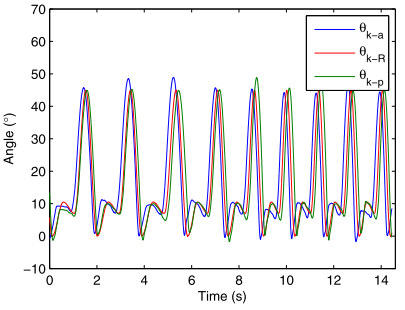


**FIGURE 18.** Time histories of the subject's knee joint's swing angle ($\theta_{k\_a}$), the knee joint reference angle ($\theta_{k\_R}$), and the prosthetic knee prototype's swing angle ($\theta_{k\_p}$) in the second walking process.

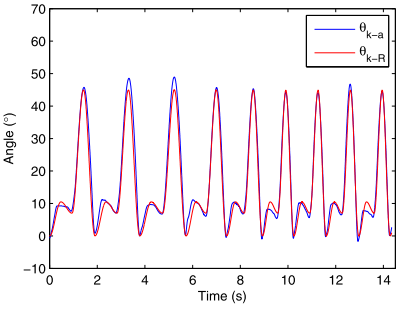


**FIGURE 19.** Time histories of the subject's knee joint's swing angle ($\theta_{k\_a}$) and the knee joint reference angle ($\theta_{k\_R}$) when ignoring the delay time in the second walking process.

0.016 s. The experimental result shows that the developed RORAG model can generate the reference angle for the prosthetic knee prototype in real time.

The delay time between the knee joint reference angle ($\theta_{k\_R}$) and the prosthetic knee prototype's swing angle ($\theta_{k\_p}$) is about 0.036 s. So the delay time between the thigh simulator's swing angle ($\theta_{t\_p}$) and the prosthetic knee prototype's swing angle ($\theta_{k\_p}$) is about 0.052 s. Because the response time of the human body is approximately between 0.15 s and 0.40 s [35], the knee joint reference angle ($\theta_{k\_R}$) generated by the RORAG model can achieve the synchronization between the thigh simulator's swing angle ($\theta_{t\_p}$) and the prosthetic knee prototype's swing angle ($\theta_{k\_p}$). It should be note that the delay time in Figures 15 and 18 is caused by both the

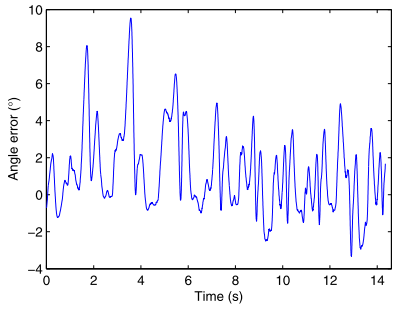


**FIGURE 20.** Time histories of the angle error between the subject's knee joint's swing angle ($\theta_{k\_a}$) and the knee joint reference angle ($\theta_{k\_R}$) in the second walking process.

calculation time of the controller and the response time of the actuator. Therefore, the delay time cannot be compensated by the RORAG algorithm. The delay time could be reduced by using both the controller with faster calculation speeds and the actuator with shorter response time, but it cannot be completely eliminated.

According to Figures 16 and 17, in the first walking process, the maximum absolute angle error between the knee joint reference angle ($\theta_{k\_R}$) and the subject's knee joint's swing angle ($\theta_{k\_a}$) is 10.39 °, the maximum relative angle error is 23.09 %, and the RMSE is 2.96 °. According to Figures 19 and 20, in the second walking process, the maximum absolute angle error between the knee joint reference angle ($\theta_{k\_R}$) and the subject's knee joint's swing angle ($\theta_{k\_a}$) is 9.54 °, the maximum relative angle error is 21.20 %, and the RMSE is 2.53 °. In each of the two experiments, the RMSEs between the knee joint reference angle ($\theta_{k\_R}$) and the subject's knee joint's swing angle ($\theta_{k\_a}$) are both less than 3 °. The experimental result shows that the knee joint reference angle ($\theta_{k\_R}$) generated by the RORAG model can accurately imitate the subject's knee joint's swing angle ($\theta_{k\_a}$).

According to the analysis of the above experimental results, the developed RORAG model can imitate the swing angle of the subject's knee joint accurately in real time. Therefore, the proposed RORAG is effective in practical applications.

## V. CONCLUSION

In order to synchronize the motions of the above-knee amputee's limbs and smart prosthetic knee in practical applications, the principle of the RORAG for motion control of smart prosthetic knees is proposed. The specific contributions of this work are: (1) a reference angle generator, whose parameters are corresponding to the motion characteristics of biological lower limb, is realized by improving a pair of phase-coupling Rayleigh oscillators; (2) the synchronization between the established CPG model and the above-knee amputee's limb's biological CPG is realized. A frequency control method for the lower limb's CPG model is proposed to synchronize the frequency of the thigh reference angle generated by the CPG model with the swing frequency of the above-knee amputee's residual thigh; (3) the corresponding experimental system is specially developed and fabricated to verify the effectiveness of the proposed RORAG in practical applications. The RORAG model is developed by using the real-time simulation system. An experimental system is established to verify the RORAG model in two terms of the curve shape and motion synchronization. Further, a bio-guided motion platform system is developed and fabricated to verify the RORAG model in two terms of the real-time and accuracy. The delay time between the knee joint reference angle ($\theta_{k\_R}$) generated by the RORAG model and the thigh simulator's swing angle ($\theta_{t\_p}$) in the motion platform system is about 0.016 s. The RMSE between the knee joint reference angle ($\theta_{k\_R}$) and the subject's knee joint's swing angle ($\theta_{k\_a}$) is less than 3 °. The experimental results show that the developed RORAG model can imitate the subject's knee joint's swing angle accurately in real time. Therefore, the developed RORAG is effective in practical applications. The proposed and developed RORAG can be effectively used for motion control of the smart prosthetic knees to promote the development of the relevant technology of the smart prosthetic knees, and has important research value and social significance.

## REFERENCES

[1] J. L. Johansson, D. M. Sherrill, P. O. Riley, P. Bonato, and H. Herr, "A clinical comparison of variable-damping and mechanically passive prosthetic knee devices," *Amer. J. Phys. Med. Rehabil.*, vol. 84, no. 8, pp. 563–575, Aug. 2005.

[2] G. Z. Tan and L. M. Wu, "Progress and development trend towards study of artificial legs (prostheses) in foreign contries and China," *Robot*, vol. 23, no. 1, pp. 91–96, 2001.

[3] B. R. Wang and X. H. Xu, "Study of intelligent bionic limb prosthesis," *Control Decis.*, vol. 19, no. 2, pp. 121–133, 2004.

[4] J. D. Carlson, W. Matthis, and J. R. Toscano, "Smart prosthetics based on magnetorheological fluids," *Smart Struct. Mater. Conf.*, vol. 4332, Newport Beach, CA, USA, Jun. 2001, pp. 308–316.

[5] D. Zlatnik, B. Steiner, and G. Schweitzer, "Finite-state control of a trans-femoral (TF) prosthesis," *IEEE Trans. Control Syst. Technol.*, vol. 10, no. 3, pp. 408–420, May 2002.

[6] T. K. Wang, M. S. Ju, and Y. G. Tsuei, "Adaptive control of above knee electro-hydraulic prosthesis," *J. Biomech. Eng.*, vol. 114, no. 3, pp. 421–424, Aug. 1992.

[7] K. E. Akdogan, A. Yilmaz, and S. Duman, "Simulations of knee angle control in dynamical gait model for above knee prosthesis," in *Proc. IEEE 17th Signal Process. Commun. Appl. Conf.*, Antalya, Turkey, Apr. 2009, pp. 822–825.

[8] D. B. Popović and V. D. Kalanovic, "Output space tracking control for above-knee prosthesis," *IEEE Trans. Biomed. Eng.*, vol. 40, no. 6, pp. 549–557, Jun. 1993.

[9] D. B. Popović, M. N. Oğuztöreli, and R. B. Stein, "Optimal control for an above-knee prosthesis with two degrees of freedom," *J. Biomech.*, vol. 28, no. 1, pp. 89–98, Jan. 1995.

[10] V. D. Kalanovic, D. Popovic, and N. T. Skaug, "Feedback error learning neural network for trans-femoral prosthesis," *IEEE Trans. Rehab. Eng.*, vol. 8, no. 1, pp. 71–80, Mar. 2000.

[11] J. H. Kim and J. H. Oh, "Development of an above knee prosthesis using MR damper and leg simulator," in *Proc. IEEE Int. Conf. Robot. Autom. (ICRA)*, vol. 4, Nov. 2001, pp. 3686–3691.

[12] G. C. Scandaroli, G. A. Borges, R. A. F. da, and F. A. D. Nascimento, "Adaptive knee joint control for an active amputee prosthesis," in *Proc. 5th Latin Amer. Robot. Symp.*, Oct. 2008, pp. 147–152.

[13] A. J. Ijspeert, "Central pattern generators for locomotion control in animals and robots: A review," *Neural Netw.*, vol. 21, no. 4, pp. 642–653, May 2008.

[14] Q. Wu, C. Liu, J. Zhang, and Q. Chen, "Survey of locomotion control of legged robots inspired by biological concept," *Sci. China Ser. F-Inf. Sci.*, vol. 52, no. 10, pp. 1715–1729, Oct. 2009.
[15] C. S. He, "The neurophysiology basis for the rhythmic movement of human body," *Phys. Med. Rehabil.*, vol. 14, no. 4, pp. 160–162, 1994.
[16] J. Conradt, "Distributed central pattern generator control for a serpentine robot," in *Proc. Int. Conf. Artif. Neural Netw.*, Istanbul, Turkey, 2003, pp. 338–341.
[17] J. Morimoto, G. Endo, J. Nakanishi, and G. Cheng, "A biologically inspired biped locomotion strategy for humanoid robots: Modulation of sinusoidal patterns by a coupled oscillator model," *IEEE Trans. Robot.*, vol. 24, no. 1, pp. 185–191, Feb. 2008.
[18] T. Zielinska, "Coupled oscillators utilised as gait rhythm generators of a two-legged walking machine," *Biol. Cybern.*, vol. 74, no. 3, pp. 263–273, Mar. 1996.
[19] R. R. Torrealba, J. Cappelletto, L. Fermín, G. Fernández-López, and J. C. Grieco, "Cybernetic knee prosthesis: Application of an adaptive central pattern generator," *Kybernetes*, vol. 41, nos. 1–2, pp. 192–205, Mar. 2012.
[20] Q. Fu, D. H. Wang, L. Xu, and G. Yuan, "A cardioid oscillator with asymmetric time ratio for establishing CPG models," *Biol. Cybern.*, vol. 112, no. 3, pp. 227–235, Jun. 2018.
[21] A. C. D. P. Filho, M. S. Dutra, and L. S. C. Raptopoulos, "Modeling of a bipedal robot using mutually coupled Rayleigh oscillators," *Biol. Cybern.*, vol. 92, no. 1, pp. 1–7, Jan. 2005.
[22] G. C. Nandi, A. J. Ijspeert, P. Chakraborty, and A. Nandi, "Development of adaptive modular active leg (AMAL) using bipedal robotics technology," *Robot. Auto. Syst.*, vol. 57, nos. 6–7, pp. 603–616, Jun. 2009.
[23] S. Mondal, A. Nandy, C. Verma, S. Shukla, N. Saxena, P. Chakraborty, and G. C. Nandi, "Modeling a central pattern generator to generate the biped locomotion of a bipedal robot using Rayleigh oscillators," in *Proc. Contemp. Comput., 4th Int. Conf. (IC3)*, Noida, India, Aug. 2011, pp. 289–300.
[24] A. Kumar, S. Erlicher, and P. Argoul, "Phase difference in lateral synchronization of pedestrian floors using a modified hybrid van der pol/Rayleigh oscillator," *Int. J. Str. Stab. Dyn.*, vol. 16, no. 8, Oct. 2016, Art. no. 1550042.
[25] P. Kumar, A. Kumar, and S. Erlicher, "A modified hybrid Van der Pol–Duffing–Rayleigh oscillator for modelling the lateral walking force on a rigid floor," *Phys. D, Nonlinear Phenomena*, vol. 358, pp. 1–14, Nov. 2017.
[26] Q. Fu, T. Luo, C. Pan, and G. Wu, "Central pattern generator–based coupling control method for synchronously controlling the two-degrees-of-freedom robot," *Sci. Progr.*, Oct. 2019, Art. no. 003685041987773, doi: 10.1177/0036850419877731.
[27] O. Beauchet, C. Annweiler, Y. Lecordroch, G. Allali, V. Dubost, F. R. Herrmann, and R. W. Kressig, "Walking speed-related changes in stride time variability: Effects of decreased speed," *J. NeuroEng. Rehabil.*, vol. 6, no. 1, p. 32, Dec. 2009.
[28] M. Toth-Tascau and D. I. Stoia, "Influence of treadmill velocity on spatio-temporal parameters of human gait," in *Proc. E-Health Bioeng. Conf. (EHB)*, 2011, pp. 1–4.
[29] A. H. Nayfeh and D. T. Mook, *Nonlinear Oscillations*. New York, NY, USA: Wiley, 1979, pp. 59–61.
[30] L. Xu, D.-H. Wang, Q. Fu, G. Yuan, and X.-X. Bai, "A novel motion platform system for testing prosthetic knees," *Measurement*, vol. 146, pp. 139–151, Nov. 2019.
[31] X.-X. Bai, F.-L. Cai, and P. Chen, "Resistor-capacitor (RC) operator-based hysteresis model for magnetorheological (MR) dampers," *Mech. Syst. Signal Process.*, vol. 117, pp. 157–169, Feb. 2019.
[32] P. Chen, X.-X. Bai, L.-J. Qian, and S.-B. Choi, "An approach for hysteresis modeling based on shape function and memory mechanism," *IEEE/ASME Trans. Mechatronics*, vol. 23, no. 3, pp. 1270–1278, Jun. 2018.
[33] X.-X. Bai and P. Chen, "On the hysteresis mechanism of magnetorheological fluids," *Front. Mater.*, vol. 6, p. 36, Mar. 2019.
[34] L. Xu, D. H. Wang, Q. Fu, G. Yuan, and L. Z. Hu, "A novel four-bar linkage prosthetic knee based on magnetorheological effect: Principle, structure, simulation and control," *Smart Mater. Struct.*, vol. 25, no. 11, 2016, Art. no. 115007.
[35] J. Z. Chen and W. H. Liao, "Design, testing and control of a magnetorheological actuator for assistive knee braces," *Smart Mater. Struct.*, vol. 19, no. 3, 2010, Art. no. 035029.

**LEI XU** was born in Weifang, Shandong, China, in 1983. He received the B.S. degree in applied physics from Yantai University, Yantai, in 2005, and the D.Eng. degree in instrument science and technology from Chongqing University, Chongqing, China, in 2016.

Since 2017, he has been with the Department of Automation, Shanxi University. His current research interests include magnetorheological damper-based knee prostheses, bio-inspired structural design and control, and smart structures and systems.

**QIANG FU** was born in Jiangxi. He received the D.Eng. degree in instrument science and technology from Chongqing University, Chongqing, China, in 2017.

He is currently with the Chongqing University of Arts and Sciences. His current research interests include magnetorheological damper-based knee prostheses, bio-inspired robot control, nonlinear oscillator-based CPG model, and smart structures and systems.